

DOI:10.17586/1023-5086-2018-85-06-71-77

Fiber bragg grating monitoring for composites in out of autoclave curing process

© 2018 **YAGE ZHAN***; **CHANGHENG FENG***; **ZIYANG SHEN***; **NABING XIE****; **HONG LIU***; **FENG XIONG*****; **SHIJIE WANG*****; **ZEYU SUN*****; **MUNUO YU*****

*College of Science, Donghua University, Shanghai 201620, People's Republic of China

**College of Mechanical Engineering, Donghua University, Shanghai 201620, People's Republic of China

***State Key Laboratory for Modification of Chemical Fibers and Polymer Materials, Donghua University, Shanghai 201620, People's Republic of China

E-mail: zhanyg@dhu.edu.cn

Submitted 07.11.2017

Temperature and strain are two of the most significant parameters in the curing process of composites. The fabrication of the strain-free temperature sensor has been completed by encapsulating fiber Bragg grating (FBG) with capillary ceramic tube. The grating string composed of a bare grating and an encapsulated grating has been embedded in the composites. The temperature and strain of the out of autoclave curing process have been monitored. In addition, the accuracy of the temperature monitoring has been proved by comparing the temperature monitoring results with common gratings, high temperature-resistant gratings and thermocouples, respectively. It is found that the high temperature-resistant gratings are more suitable for composites curing process, especially for the monitoring of out of autoclave curing process at the internal high temperature. This study provides a reference for multi-parameter monitoring by using gratings in out of autoclave curing process of composites..

Keywords: sensor, grating, multi-parameter monitoring, composites, out of autoclave.

OCIS codes: 060.3735.

Волоконные брегговские решётки для мониторинга внеавтоклавного технологического процесса изготовления композитов

© 2018 г. **YAGE ZHAN**; **CHANGHENG FENG**; **ZIYANG SHEN**; **NABING XIE**; **HONG LIU**; **FENG XIONG**; **SHIJIE WANG**; **ZEYU SUN**; **MUNUO YU**

В технологическом процессе изготовления композитов важнейшими параметрами являются температура и деформации. Создан свободный от деформаций волоконный датчик температуры посредством инкапсулирования волоконной брегговской решётки в керамическую трубку. В композит вводились свободная брегговская решётка и решётка, инкапсулированная в керамическую трубку. Проводился мониторинг температуры и деформаций во внеавтоклавном процессе технологической обработки. Точность измерений температуры была подтверждена путём сравнения результатов, полученных с применением обычных решёток, решёток, устойчивых к высоким температурам, и термопар. Показано, что решётки, устойчивые к высоким температурам, наиболее подходят для мониторинга высокотемпературных внеавтоклавных технологических процессов изготовления композитов. Результаты могут быть использованы при разработке методов многопараметрического мониторинга этих процессов.

Ключевые слова: датчик, решётка, многопараметрический мониторинг, композитные материалы, внеавтоклавный процесс.

1. INTRODUCTION

Carbon fiber reinforced resin matrix composites have excellent specific strength, specific stiffness, fatigue resistance and superior designability. Therefore, it is widely used in the fields of aerospace, automobile and construction. There are important values in monitoring the curing properties of the composites and analyzing the evolution of the temperature and the strain. In recent years, the curing process of composites has become a hot spot. The methods of the traditional temperature and strain monitoring have a greater impact on the matrix, compatibility with composites, and the accuracy of the monitoring [1].

Because of excellent electrical insulation, free from electromagnetic interference, small measured disturbance and compatibility with the matrix material and other advantages [2–3], the fiber grating sensors are more and more applied for composites curing process monitoring. There are many reports about composites monitoring with fiber grating in hot press, light curing, autoclave, RTM and other curing process at domestic and overseas. Takuhei Tsukada et al. [4] monitored the effect of different cooling rates on the residual strain of carbon fiber unidirectional laminates with fiber gratings during the curing process. M. Mulle et al. [5] explored the strain of glass fiber reinforced polypropylene laminates at different cooling rates with embedding fiber gratings in hot-press curing processes. R. Brain Jenkins et al. [6] monitoring the surface and internal temperature variation of the composites during the photo-curing process with embedding the grating array in the carbon fiber laminate. Heng Tian [7] and Wei Qin et al [8] achieved the strain monitoring of the composites in the autoclave curing process and RTM curing process with fiber grating, respectively. Parlevliet et al. [9] monitored the effect of curing shrinkage stress and curing residual stress on the composites structure with fiber gratings. However, there are few reports on the monitoring of the out of autoclave curing process.

Since the 21st century, more and more high-level space activities have been completed, which partly due to the penetration and development of the technology of the aeronautical composite materials. The autoclave process can manufacture the high performance composites with excellent compactness, high interlaminar strength, good evenly distribution of the resin and fiber, high fiber content and low porosity. It meets the demand of the aerospace high-end application and plays an important role in promoting the development of composite materials [10]. However, because of the enlargement of the aeronautical composites and the growing problem of the resources, energy and global environment, the autoclave process has shown some disadvantages: 1) high cost of equipment; 2) high energy consump-

tion of the process; 3) low equipment utilization rate; 4) difficult control with the temperature and pressure of the large autoclave; 5) high pressure during the autoclave curing which not only increase the requirement of the material and manufacture of the die, but also increase the cost of the operation.

As the maximization and super-large of the structure are the important trend of the development of the aeronautical composite materials, the technology of the out of autoclave curing and molding, especially the technology of the vacuum bag, is increasingly favored by aeronautical manufacturers. It makes the low-cost manufacture of the maximization and super-large possible and led to the development of the corresponding material and the molding technology [11]. The technology of the out of autoclave is expected to bring new changes in aeronautical composites manufacturing.

Therefore, we try to use optical fiber Bragg grating to monitor the vacuum bag process of the composites, in which the temperature and strain are the two important parameters to be monitored. Since common fiber Bragg gratings are sensitive to temperature and strain [12–14], it is necessary to distinguish temperature and strain effects. In this paper, the Bragg grating string composed of a bare grating and an encapsulated ceramic tube is embedded in the prefabricated carbon fiber/epoxy resin laminated structure to monitor the temperature and strain during the curing process in real time. In addition, the temperature monitoring results of the common fiber Bragg grating and the high temperature-resistant fiber Bragg grating have been compared.

2. EXPERIMENTAL PRINCIPLE

Fiber Bragg grating, which formed with the ultraviolet laser and the fiber photo-sensitivity in the region of the core, is an optical structure that the refractive index is periodically changed. When the broadband light is transmitting in the fiber, the light satisfying the following condition will be reflected

$$\lambda_B = 2n_{\text{eff}}\Lambda, \quad (1)$$

where λ_B is the center reflected wavelength of the grating, n_{eff} is the effective refractive index of the core, Λ is the period of the grating. Equation (1) indicates that λ_B will change linearly with the Λ and/or n_{eff} . Λ and/or n_{eff} always change caused by the variations of temperature and/or strain of the fiber grating.

The relationship between the variation of the wavelength and the variation of the temperature/strain is

$$\Delta\lambda_B = \lambda_B[(1 - P_\varepsilon)\Delta\varepsilon + (\alpha_f + \xi)\Delta T] = K_\varepsilon\Delta\varepsilon + K_T\Delta T, \quad (2)$$

where $\Delta\lambda_B$ is the wavelength shift of the grating. P_ε is the elasto-optic coefficient of the fiber.

α_f is the thermal expansion coefficient of the fiber. ξ is the thermo-optical coefficient of the fiber. K_ε is the strain sensitivity coefficient of the grating. K_T is the temperature sensitivity coefficient of the grating. It shows that fiber Bragg grating is sensitive to both temperature and strain.

The grating string referred to the paper is composed of a bare grating (FBG1) and a strain-free grating encapsulated with a ceramic tube (FBG2). The center reflected wavelength shift of both can be expressed as

$$\begin{aligned}\Delta\lambda_{B1} &= K_{\varepsilon1}\Delta\varepsilon + K_{T1}\Delta T, \\ \Delta\lambda_{B2} &= K_{T2}\Delta T,\end{aligned}\quad (3)$$

where $\Delta\lambda_{B1}$ is the wavelength shift of the FBG1 and $\Delta\lambda_{B2}$ is the central wavelength shift of the FBG2. K_{T1} and $K_{\varepsilon1}$ are the temperature sensitivity coefficient and strain sensitivity coefficient of the FBG1, respectively. K_{T2} is the temperature sensitivity coefficient of the FBG2.

The amount of variation about the temperature and the strain can be deduced according to equation (3), shown in the following equation (4):

$$\begin{aligned}\Delta\varepsilon &= (\Delta\lambda_{B1}K_{T2} - \Delta\lambda_{B2}K_{T1})/(K_{T2}K_{\varepsilon1}), \\ \Delta T &= \Delta\lambda_{B2}/K_{T2}.\end{aligned}\quad (4)$$

According to the wavelength shifts and the temperature/strain sensitivity coefficients of the two gratings, the measured temperature and strain can be calculated.

Fig. 1a and Fig. 1b are the structure diagrams of the bare grating FBG1 and the encapsulated grating FBG2 respectively. Due to the cross-sensitivity of the FBG1, the FBG2 is embedded near FBG1 for temperature compensation. FBG2 is pre-stretched before it is encapsulated into the capillary ceramic tube, which improve the monitoring range especially when the FBG subjected to the compressive stress. Both ends of the capillary ceramic tube are sealed with HZ8811 two-component epoxy resin adhesive to the acrylate external envelope and allowed to leave at room temperature for 24 hours for fully curing.

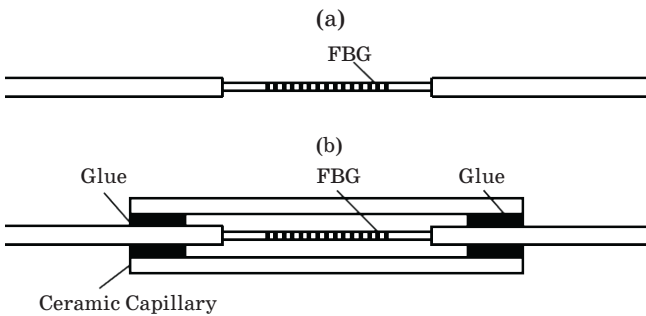


Fig. 1. The structures of FBG sensors. The bare grating sensor (a), the encapsulated grating sensor (b).

3. EXPERIMENTAL PROGRAM

3.1. Grating paving program

The composites are fabricated with the Dongli UA2433-125 carbon fiber unidirectional prepreg and the thickness of prepreg is 0.1 mm. The laminates are designed in dimensions 300×200 mm and the stacking sequence is $[0^\circ]_{10}$. 5 positions have been designed as the candidate embedded points for gratings, shown in Fig. 2.

In order to study the monitoring performances of the gratings during the out of autoclave curing process, three series of experiments have been carried out. The temperature and strain sensitivity coefficients of the gratings have been measured and calibrated before the experiments. All the gratings were embedded between the 5th and 6th layers. The laying direction of the gratings was 0° . In the first series of experiments, two grating strings were embedded at position 1 and position 2 respectively. In the second series of experiments, a high temperature-resistant grating and a thermocouple were embedded at position 2. Another thermocouple was embedded at position 3 and a grating string was embedded at position 5. The direction of the thermocouple was parallel to the grating direction. In the third series of experiments, a grating string was embedded at position 4. A high temperature-resistant grating and a thermocouple were embedded at position 5.

3.2. Curing and monitoring programs

The vacuum bag process has been used for curing and the oven has been used for heating. The curing process is divided into five stages: 1) preheating stage: the oven environmental temperature rises from room temperature to 90°C ; 2) the first isothermal stage: the temperature is isothermally treated for 0.5 hours with 90°C ; 3) heating stage: The environmental temperature rises from 90°C to 120°C ; 4) the second isothermal stage: the temperature is isothermally treated for 1 hours with 120°C ; 5) cooling stage: natural cooling. The curing negative pressure of the vacuum bag is -0.099 MPa . The FBG wavelength demodulator is MOI SM125 with the sampling frequency of 1 Hz and wavelength accuracy

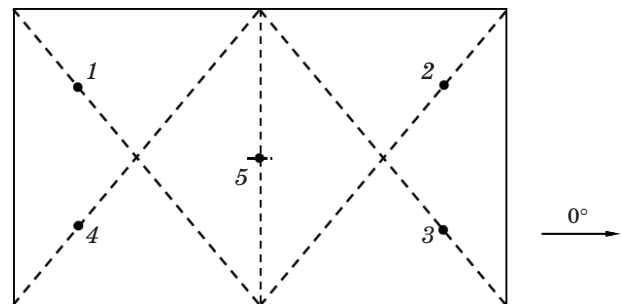


Fig. 2. 5 candidate embedded points for gratings.

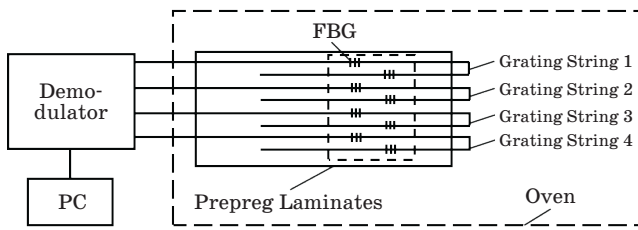


Fig. 3. The diagram of the monitoring during the out of autoclave curing process.

of 1 pm. The experimental setup is shown in Fig. 3. The demodulator can simultaneously demodulate the grating wavelengths in series on the four channels shown in the Fig. 3.

4. EXPERIMENTAL RESULTS AND ANALYSIS

4.1. The results of the first series of experiments

The grating temperature monitoring results of the first series of experiments have been shown in Fig. 4. It can be seen that the monitored internal temperature of the laminates is not exactly the same as the environmental temperature in the oven. The reason perhaps is that a glass carrier is used in the experiment and its heat conduction is slower compared with the metal carrier. It makes the temperature rise and cool slowly which results in a certain delay. Therefore, the glass carrier temperature is still rising in the second isothermal stage. The environmental temperature in the oven began to decrease at about 130 minutes, however, the carrier temperature began to decrease from about 140 minutes. The experimental results show that the material of the carrier should be selected as the metal carrier with better heat conduction performance when the composites are curing.

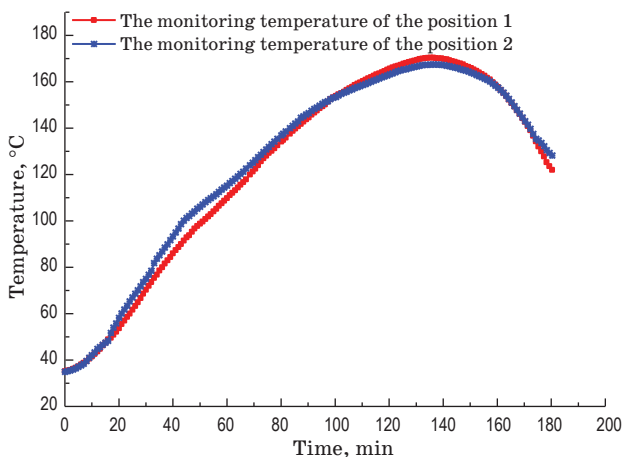


Fig. 4. The grating temperature monitoring results of the first series of experiments.

The grating strain monitoring results of the first series of experiments have been shown in Fig. 5. The strain of the position 1 and 2 firstly decreases and rises again before 90 minutes, secondly decreases during 90–140 minutes and finally increases after 140 minutes.

Before 90 minutes, the temperature rising of the prepreg was slow because of the glass carrier. When the system temperature began to rise, the resin viscosity decreased, the mobility of the resin enlarged, and the resin contracted due to partial resin cross-linking. Increased compressive stress resulted in reduced strain. The temperature reached 90 °C at about 40 minutes, which is the gel point. As the environmental temperature in the oven rose continuously, the carbon fibers were stretched and the tensile stress increased, which resulted in the increased strain. After 90 minutes in Fig. 5, the resin under the viscous fluid state gradually converted to viscoelastic solid state when the curing cross-linking reaction of the resin system progressed continuously. At this time the volume shrinkage caused by the further crosslinking of the resin mainly resulted in the compressive stress of the whole system. The pressure of the fiber was reduced and the tensile stress of the grating was also reduced. For position 1 and 2 in Fig. 5, the compressive stress increased continuously during 90–140 minutes, which indicated that the curing has been converted from a viscous fluid state to a viscoelastic solid state. The whole system was in the curing reaction stage and the compressive stress of the FBG strain sensor increased caused by the curing shrinkage. After the end of the curing reaction at about 140 minutes, the temperature of the whole system gradually decreased and residual strain caused by curing was gradually released, which resulting in the strain of the position 1 increased and the strain of the position 2 gradually restored.

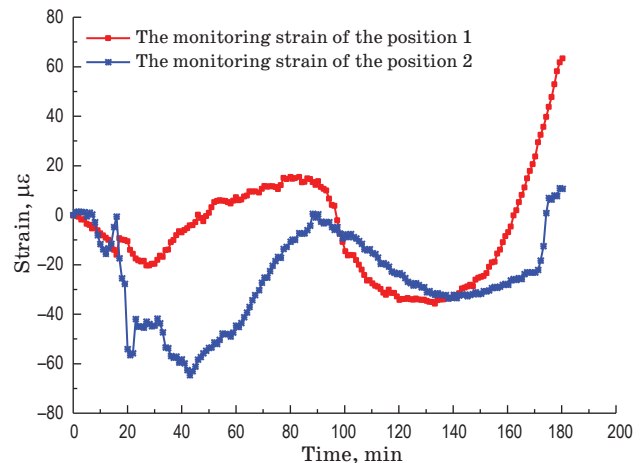


Fig. 5. The grating strain monitoring results of the first series of experiments.

4.2. The monitoring results of the second series of experiments

As the wavelength of the grating changes linearly with the temperature and the strain. If the wavelength shift due to one of the parameters (such as temperature) can be distinguished from the overall wavelength shift and this part of the wavelength shift can be proved accurate, when this partial shift is separated from the total shift, the result is the wavelength shift caused by another parameter (such as strain). According to the two separated wavelength shift, the temperature and strain could be calculated and measured.

The thermocouple has been used to verify the temperature monitoring accuracy of the gratings in the second series of experiments, the thermocouples with a diameter of 0.2 mm were embedded at position 2 and position 3, and the gratings were embedded at position 2 and 5. The results of the second series of experiments have been shown in Fig. 6.

In Fig. 6, the monitoring results of each FBG temperature sensor agree basically with each other with the maximum difference of 2 °C, which shows that the temperature difference between the different positions of composite laminates is small. There is a good consistency between the grating monitoring results and the thermocouple temperature measurement results with the maximum difference of 2.5 °C. These results show that the temperature monitoring with the grating during the composites curing process is accurate.

The grating strain monitoring results of the second series of experiments have been shown in Fig. 7. The strain of the position 5 monitored in this series were collected from the center of the laminates. There is an offset between the shrinkage stress caused by the contraction of the carbon fiber and the partial tensile stress caused by the fiber stretching due to the symmetry of the structure. However, the impact

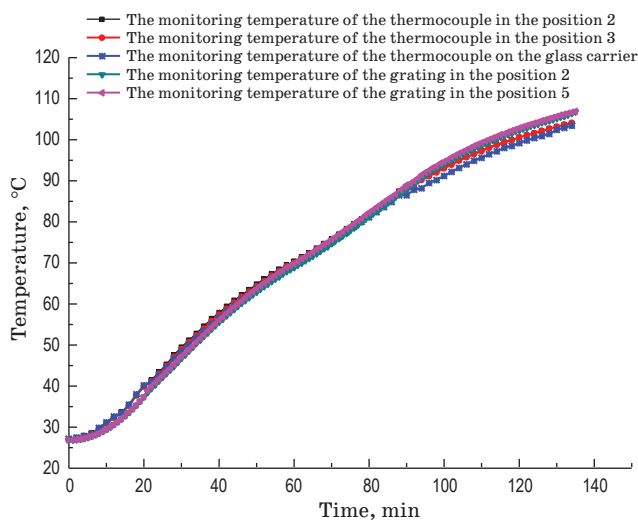


Fig. 6. The grating temperature monitoring results of the second series of experiments.

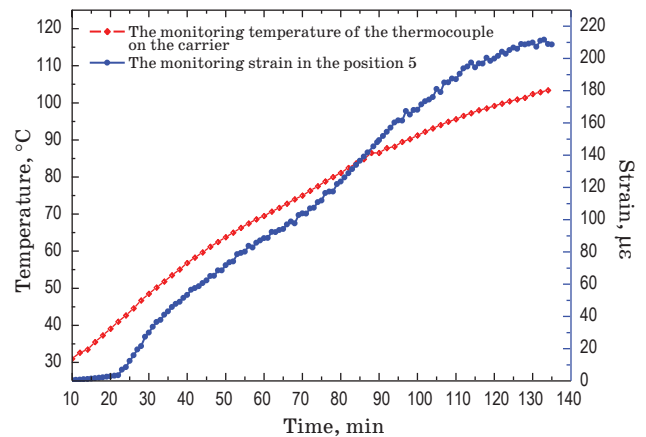


Fig. 7. The grating strain monitoring results of the second series of experiments.

of the tensile stress was significant. Therefore, the tensile stress before 140 minutes increased continuously, as shown in Fig. 7.

4.3. The monitoring results of the third series of experiments

The grating temperature monitoring results of the third series of experiments have been shown in Fig. 8. Analyzing the results of the common grating embedded at position 5 and the results of the high temperature-resistant grating embedded at position 4, it is indicated that the temperature of the high temperature-resistant grating coincides with the thermocouple temperature results. However, there is a difference between the temperature monitored with common grating and the temperature monitored with the thermocouple. It is shown that the sensing performance of the high temperature-resistant gratings is better than that of the common grating, under the same experimental conditions. The high temperature-resistant gratings can moni-

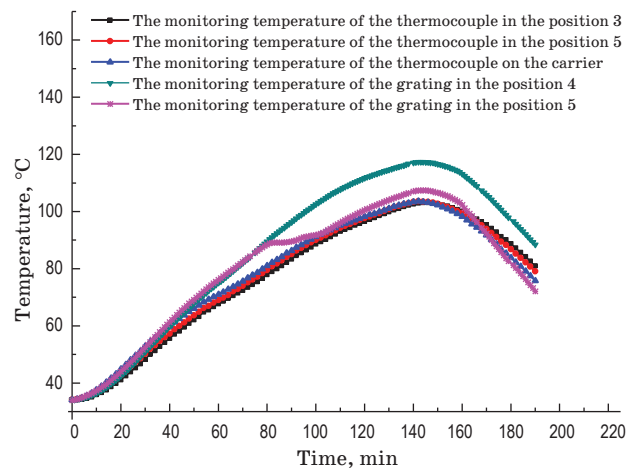


Fig. 8. The grating temperature monitoring results of the third series of experiments.

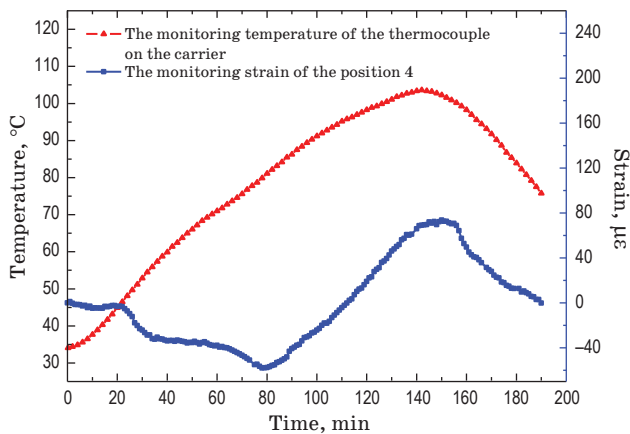


Fig. 9. The grating strain monitoring results of the third series of experiments.

tor the real temperature more accurately in the curing of the prepreg.

The grating strain monitoring results of the third series of experiments have been shown in Fig. 9. The strain of the position 4 firstly decreases instability and then rises before 150 minutes, and finally decreases after 150 minutes.

Before 150 minutes, the strain variation was related to two effects. One effect is the contraction due to partial crosslinking of the resin and the other is volume expansion due to the temperature rising. The temperature reached 90 °C at about 100 minutes, which is the gel point. After 150 minutes, the resin from the viscous fluid state converted gradually into viscoelastic solid state with the curing cross-linking reaction of the resin system progressed continuously. Then the resin of the whole system crosslinks further which results in the volume shrinkage and the reduction of fiber pressure.

In Fig. 9, the compressive stress at position 4 increased at about 150–160 minutes, indicating that the curing has been converted from the viscous fluid state to the viscoelastic solid state. The whole system is in the curing reaction stage. Because of the curing shrinkage, the FBG strain sensor is subjected to the compressive stress. After the curing reaction, the temperature of the whole system decreased gradually and the residual strain was released. The whole system was in a recovery state, while the strain of the position 4 became zero gradually.

REFERENCES

1. Hadzica R., Johna S., Herszberg I. Structural integrity analysis of embedded optical fibres in composite structures // *Compos. Struct.* 1999. V. 47. № 12. P. 759–765.
2. Majumder M., Gangopadhyay T.K., Chakraborty A.K., Dasgupta K., Bhattacharya D.K. Fibre Bragg gratings in structural health monitoring-present status and applications // *Sensor. Actuat. A-phys.* 2008. V. 147. № 9. P. 150–164.
3. Kim S.-W. Characteristics of strain transfer and the reflected spectrum of a metal-coated fiber Bragg grating sensor // *Opt. Laser. Eng.* 2017. V. 96. № 9. P. 83–93.

5. CONCLUSION

A strain-free temperature sensor has been fabricated by encapsulating the fiber Bragg grating with capillary ceramic tube. Comparing the temperature measurement results of the thermocouples and the results of the common gratings, it is shown that the scheme using gratings for monitoring the composites internal temperature during the curing process is accurate. The composites internal strains during the out of autoclave curing process have been explored, which provides a reference for the application of the fiber gratings for two-parameter (temperature and strain) monitoring during the out of autoclave curing process of composites.

For temperature measurement, it is found that the high temperature-resistant gratings during the curing process at all temperature stages can accurately reflect the internal temperature of composites, by comparing the results of the high temperature-resistant gratings with the results of thermocouple, under the same experimental conditions. The common gratings are more reliable only at low temperature. However, there is a partly difference between the results monitored at high temperature and the real temperature inside the composites. It is confirmed that the high temperature-resistant gratings are more suitable to temperature monitoring during the out of autoclave curing process.

Fiber Bragg grating monitoring for composites in out of autoclave curing process can obtain the internal temperature and strain of the laminates. The curing process can be adjusted according to the monitored internal temperature and strain of the laminates in time, which ensure the optimizing curing conditions to the composites. Therefore, the quality of the thermosolidified composite materials product can be improve with the fiber Bragg grating monitoring for composites in out of autoclave curing process.

The development supported by National Engineering Research Center, Shanghai Aircraft Manufacturing Co. Ltd (COMAC-SFGS-2016-33236), Nonlinear Science Institute Donghua University, and the Fundamental Research Funds for the Central Universities (Project of the State Key Laboratory for Modification of Chemical Fibers and Polymer Materials, Donghua University, 17D128105).

4. *Tsukada T., Takeda S.-i., Minakuchi S., Iwahori Y., Takeda N.* Evaluation of the influence of cooling rate on residual strain development in unidirectional carbon fibre/polyphenylenesulfide laminates using embedded fibre Bragg grating sensors // *J. Compos. Mater.* 2017. V. 51. № 7. P. 1849–1859.
5. *Mulle M., Wafai H., Yudhanto A., Lubineau G., Yaldiz R., Schijve W., Verghese N.* Process monitoring of glass reinforced polypropylene laminates using fiber Bragg gratings // *Compos. Sci. Technol.* 2016. V. 123. № 2. P. 143–150.
6. *Jenkins R.B., Joyce P., Mechtel D.* Localized temperature variations in laser-irradiated composites with embedded fiber Bragg grating sensors // *Sensors-basel.* 2017. V. 17. № 2. P. 251.
7. *Tian H., Wang J., Ji Y.D., Ye C.S., Hu H.X.* The monitoring of cure-induced residual stress by fiber Bragg grating sensors // *Materials review.* 2012. V. 26. № 10. P. 111–114.
8. *Qin W., Wu X.H., Cao M.S.* Monitoring for residual strain of resin cure during the process of RTM composites // *Journal of Aeronautical Materials.* 2005. V. 25. № 4. P. 50–52.
9. *Parlevliet P.P., Bersee H.E.N., Beukers A.* Measurement of (post-)curing strain development with fiber Bragg gratings // *Polym. Test.* 2010. V. 29. № 3. P. 291–301.
10. *Grunenfeldera L.K., Dillsb A., Centeab T., Nutta S.* Effect of prepreg format on defect control in out-of-autoclave processing // *Compos. Part. A-Appl. S.* 2017. V. 93. № 2. P. 88–99.
11. *Centea T., Grunenfelder L.K., Nutt S.R.* A review of out-of-autoclave prepregs-material properties, process phenomena, and manufacturing considerations // *Compos. Part. A-Appl. S.* 2015. V. 70. № 3. P. 132–154.
12. *Sengupta S., Ghorai S.K., Biswas P.* Design of superstructure fiber Bragg grating with efficient mode coupling for simultaneous strain and temperature measurement with low cross-sensitivity // *IEEE. Sens. J.* 2016. V. 16. № 11. P. 7941–7949.
13. *Zhao Y., Gu Y.F., Lv R.Q., Yang Y.* A small probe-type flowmeter based on the differential fiber Bragg grating measurement method // *IEEE. T. Instrum. Meas.* 2017. V. 66. № 3. P. 3.
14. *Li T.L., Tan Y.G., Han X., Zheng K., Zhou Z.D.* Diaphragm based fiber Bragg grating acceleration sensor with temperature compensation // *Sensors-basel.* 2017. V. 17. № 1. P. 218.